

## Research Article

Yuan She\*, Chong Zou\*, Shiwei Liu, Keng Wu, Hao Wu, Hongzhou Ma, and Ruimeng Shi

# Combustion and gasification characteristics of low-temperature pyrolytic semi-coke prepared through atmosphere rich in CH<sub>4</sub> and H<sub>2</sub>

<https://doi.org/10.1515/gps-2021-0015>

received November 09, 2020; accepted January 24, 2021

**Abstract:** Thermoanalysis was used in this research to produce a comparative study on the combustion and gasification characteristics of semi-coke prepared under pyrolytic atmospheres rich in CH<sub>4</sub> and H<sub>2</sub> at different proportions. Distinctions of different semi-coke in terms of carbon chemical structure, functional groups, and micropore structure were examined. The results indicated that adding some reducing gases during pyrolysis could inhibit semi-coke reactivity, the inhibitory effect of the composite gas of H<sub>2</sub> and CH<sub>4</sub> was the most observable, and the effect of H<sub>2</sub> was higher than that of CH<sub>4</sub>; moreover, increasing the proportion of reducing gas increased its inhibitory effect. X-ray diffractometer and Fourier-transform infrared spectrometer results indicated that adding reducing gases in the atmosphere elevated the disordering degree of carbon microcrystalline structures, boosted the removal of hydroxyl- and oxygen-containing functional groups, decreased the unsaturated side chains, and improved condensation degree of macromolecular networks. The nitrogen adsorption experiment revealed

that the types of pore structure of semi-coke are mainly micropore and mesopore, and the influence of pyrolytic atmosphere on micropores was not of strong regularity but could inhibit mesopore development. Aromatic lamellar stack height of semi-coke, specific surface area of mesopore, and pore volume had a favorable linear correlation with semi-coke reactivity indexes.

**Keywords:** coal pyrolysis, semi-coke, blast furnace injection, reactivity, pore structure

## 1 Introduction

Low-temperature pyrolytic semi-coke is a solid product after removing a number of volatiles from low-rank coal under low-temperature pyrolysis (500–600°C) and tar is separated out [1,2]. Part of this product has been applied to fields like coal gasification, ferroalloy smelting, and calcium carbide production; however, there is still a large quantity of semi-coke resources that require market consumption. In the field of iron-making, pulverized coal injection (PCI) in blast furnace replaces expensive and highly deficient metallurgical coke with relatively low-priced coal to reduce the coke ratio in the blast furnace during iron-making process, and thereby reduce pig iron cost [3,4]. With the continuously increasing blast furnace injection ratio, iron and steel enterprises have an increasing demand for anthracite. Moreover, anthracite reserves only occupy 10.9% of coal reserves in China with unceasingly prominent scarcity, which is then accompanied by rising price. Therefore, under the background of an increase in PCI ratio in blast furnace, seeking for new low-cost and high-quality injecting fuels such as biochar [5] and waste plastics [6] has always been a research emphasis of metallurgists. Using low price semi-coke as PCI fuel to replace expensive anthracite has been an important research orientation for optimizing blast furnace fuel structures, and the reduced production cost has attracted attention from metallurgists [7–11]. Semi-coke

\* Corresponding author: Yuan She, School of Metallurgical and Ecological Engineering, University of Science and Technology Beijing, 30 Xueyuan Road, Beijing 100083, China; School of Metallurgical Engineering, Xi'an University of Architecture and Technology, 13 Yanta Road, Xi'an 710055, China,  
e-mail: sheyuan1982@163.com

\* Corresponding author: Chong Zou, School of Metallurgical Engineering, Xi'an University of Architecture and Technology, 13 Yanta Road, Xi'an 710055, China, e-mail: zouchong985@163.com  
Shiwei Liu: School of Metallurgical Engineering, Xi'an University of Architecture and Technology, 13 Yanta Road, Xi'an 710055, China, e-mail: liushiw2010@126.com

Keng Wu: School of Metallurgical and Ecological Engineering, University of Science and Technology Beijing, 30 Xueyuan Road, Beijing 100083, China

Hao Wu, Hongzhou Ma, Ruimeng Shi: School of Metallurgical Engineering, Xi'an University of Architecture and Technology, 13 Yanta Road, Xi'an 710055, China

is a potential excellent blast furnace fuel by virtue of favorable transport performance, high calorific value, and no explosiveness [7,10]. However, compared with anthracite, the nature difference of semi-coke is considerable because of its instable quality; moreover, the fluctuation of its combustion performance is remarkable and hinders its application and promotion in blast furnace injection, because during semi-coke production, pyrolysis conditions will influence the semi-coke composition and structure and cause changes in its reactivity. Even if the same coal category is used as a pyrolytic raw material, the reactivity of prepared semi-coke will be critically different, and high pyrolysis degree is adverse to follow-up combustion of semi-coke [11,12]. Factors, such as devolatilization behavior, pore structure, specific surface area, and ordering degree of carbon lattice structure, will result in substantial loss of semi-coke reactivity [13–15]. Combustion reactivity in later phase of semi-coke under high temperature is closely related to semi-coke nature before combustion [16].

The present industrialized pyrolytic processes generally use internal heating-type gas-carrier pyrolysis reactors. In such pyrolysis environments, the raw coal exists not in a pure  $N_2$  atmosphere but in mixed reducing gases such as  $CO$ ,  $H_2$ , and  $CH_4$ . Moreover, pyrolysis atmosphere contents are different to a certain degree at various positions inside the furnace. The influences of pyrolysis conditions, such as pyrolysis temperature, heating rate, atmosphere pressure, and holding time, on semi-coke composition, structure, and reactivity [17–19] have been extensively studied; however, the effects of pyrolytic atmosphere on semi-coke reactivity remain controversial. Colette *et al.* [20,21] studied the influence of the coke-oven gas atmosphere on product distribution and semi-coke characteristics in fixed beds and found that semi-coke combustion characteristics were not eminently different under  $H_2$  and inert atmospheres. Liao *et al.* [22] indicated that the combustion reactivity of coal-coke-oven gas co-pyrolytic semi-coke is related to pyrolysis pressure and heating rate, and that low pyrolysis pressure and high heating rate contribute to semi-coke combustion reactivity. Zhong *et al.* [23] found that hydrogen-free radicals generated by  $H_2$  and  $CH_4$  could permeate semi-coke and influence its oxidizing reactivity. Thus, the influence of mixed atmospheres containing reducing gases on semi-coke nature and its reactivity requires further research.

During iron-making technology in blast furnace, PCI fuels experience processes, such as volatile extrusion and combustion and gasification of fixed carbon, within confined spaces in the tuyere and raceway region. Compared with the process of release and combustion of volatiles,

char combustion and gasification are relatively slow (20 ms vs 1–4 s), and the time needed for a complete reaction of coal is primarily and jointly determined by char combustion and gasification time [24]. Combustion and gasification properties are highly important for the utilization ratio of fuels inside the furnace and the stable operation of the blast furnace because the combustion of atmosphere inside the hearth is gradually variational. In the front of the tuyere, generated coal gas components are different because of different combustion conditions at different positions along the hearth radius in front of the tuyere.  $O_2$  is sufficient in front of the tuyere and reacts with fuel combustion to generate a large quantity of  $CO_2$ ,  $O_2$  abruptly decreases and disappears, and  $CO_2$  rapidly rises to its maximum value. Therefore, the injected fuel first experiences atmospheric combustion with sufficient  $O_2$  and then experiences gasification under the atmosphere with a continuously rising  $CO_2$ . However, many research on reactivity of PCI fuels only focuses on combustion reactivity [3,25,26] and neglects the importance of gasification reactivity on the consumption of unburned char; moreover, comparative studies on the two above-mentioned subject matter are lacking.

In the present research, thermoanalysis was applied to comparatively study the combustion and gasification reactivity of semi-coke prepared under pyrolytic atmospheres containing different proportions of  $H_2$ - and  $CH_4$ -reducing gases. Moreover, the relationships between semi-coke composition/structure and combustion/gasification reactivity were obtained by analyzing the carbon chemical structures of different semi-coke, functional group analysis, and micro-pore structures to provide reference for further scientific and highly efficient application of semi-coke in PCI.

## 2 Experimental procedure

### 2.1 Experimental raw materials

Coal samples used in the experiment were typical low-rank coals from Sunjiacha coal mine in Shenmu region of Northern Shaanxi. Proximate analysis and element analysis of coals are illustrated in Table 1. Vertical-type pyrolyzing furnace was used to prepare semi-coke samples, and the pyrolysis system is shown in Figure 1. A total of 250 g samples with granularity within 20–40 mm was placed in a furnace and suspended on an electronic scale. A total of six pyrolytic atmospheres (respectively being (1) pure  $N_2$ ; (2) 10%  $CH_4$  in  $N_2$ ; (3) 20%  $CH_4$  in  $N_2$ ; (4) 10%

**Table 1:** Proximate analysis and ultimate analysis of coal and chars

Samples	Proximate analysis (wt%, ad)				Ultimate analysis (wt%, ad)				
	$M_{ad}$	$A_{ad}$	$V_{daf}$	FC	C	H	N	O	S
Coal	3.83	7.53	37.06	55.97	71.97	4.08	0.93	10.21	0.20
char1	1.17	9.15	8.21	81.47	82.8	2.42	0.61	1.17	0.23
char2	1.38	9.99	8.04	80.59	83.71	2.02	0.38	1.38	0.20
char3	1.44	8.23	8.01	82.32	83.09	1.87	0.28	1.44	0.21
char4	1.40	9.01	8.49	81.10	82.81	2.24	0.55	1.34	0.16
char5	1.32	8.99	7.40	82.29	83.45	2.01	0.62	1.26	0.19
char6	1.23	8.40	7.11	83.26	83.02	1.95	0.51	1.31	0.17

$H_2$  in  $N_2$ ; (5) 20%  $H_2$  in  $N_2$ ; and (6) 10%  $H_2$ , and 10%  $CH_4$  in  $N_2$ ) were pumped into the reaction jar at a 0.6 L/min flow rate. Samples were heated to 600°C at a rate of 5°C/min and heat was preserved for 30 min, then nitrogen was pumped in for cooling in room temperature. After pyrolysis, semi-coke samples were extracted, labeled char1–char6, and preserved in a drying vessel for further property analysis. The detailed properties of the samples are summarized in Table 1.

## 2.2 Representation of semi-coke properties

Combustion and gasification reactivity of semi-coke with an experimental weight of  $10 \pm 0.1$  mg was tested using STA449C thermal analyzer from German NESZCH company. Under atmosphere of air (combustion)/ $CO_2$  (gasification) and a flow rate of 50 mL/min, the temperature was elevated from room temperature to 1,000°C (combustion)/1,400°C (gasification) at a rate of 15°C/min, and weight change was synchronously recorded. For the quantitative comparison of semi-coke reactivity, the

combustion reactivity index  $R_c$  and gasification reactivity index  $R_g$  were introduced [27,28]:

$$R_c = \frac{V_{\text{rate}}}{T_{\text{ignition}}}, \quad (1)$$

$$R_g = \frac{0.5}{t_{0.5}}, \quad (2)$$

where  $V_{\text{rate}}$  is the average reaction rate of semi-coke combustion,  $T_{\text{ignition}}$  is the ignition point of semi-coke combustion determined through thermogravimetry-derivative thermogravimetry (TG-DTG) method [29], and  $t_{0.5}$  is the time for carbon conversion rate  $\alpha$  to reach 50%.  $\alpha$  was determined using:

$$\alpha_i = \frac{w_0 - w_i}{w_0 - w_{\text{ash}}}, \quad (3)$$

where  $w_0$  is the initial semi-coke mass,  $w_i$  is the semi-coke mass at any time, and  $w_{\text{ash}}$  is the ash content mass in the semi-coke.

Carbon chemical constitution of semi-coke was measured through X-ray diffractometer (XRD) (X'Pert PROMPD)

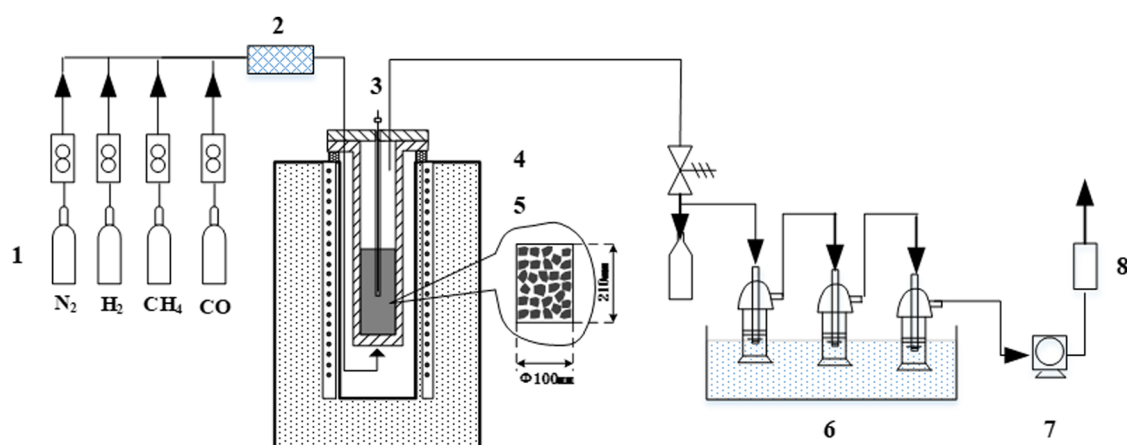


**Figure 1:** Pyrolysis device diagram. (1) Gas cylinder; (2) gas blending instrument; (3) sample temperature thermocouple; (4) temperature thermocouple inside furnace; (5) pyrolyzing furnace; (6) gas purification and tar collection; (7) pump; (8) gas analyzer.

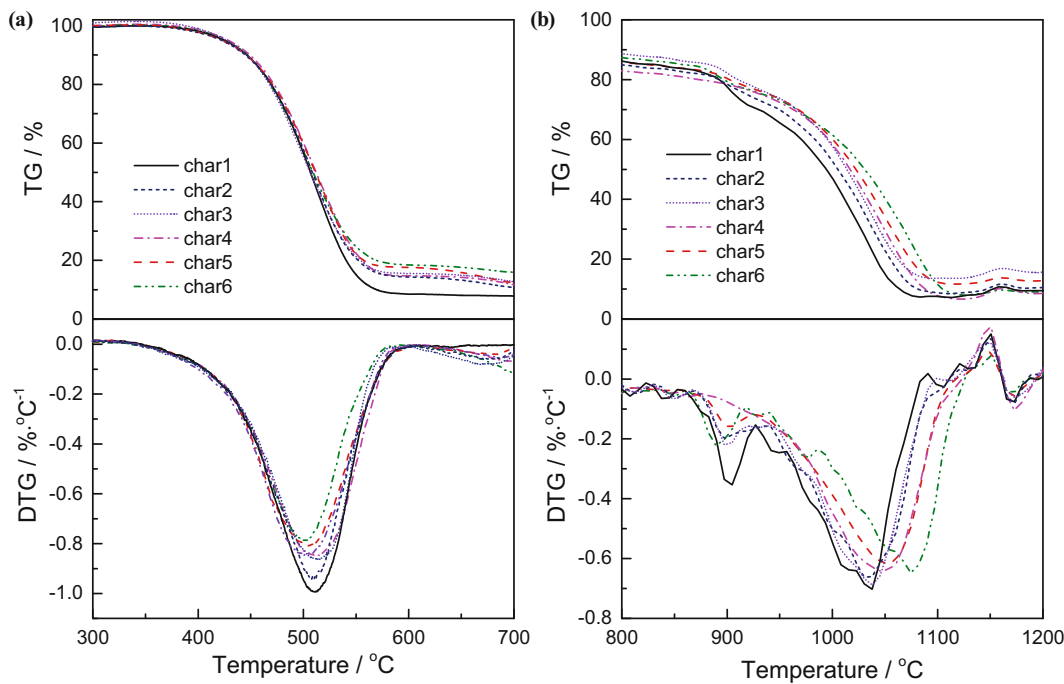


**Figure 2:** TG–DTG curves of combustion and gasification processes of semi-coke samples prepared under different pyrolytic atmospheres. (a) Air atmosphere; (b)  $\text{CO}_2$  atmosphere.

using Cu- $\text{K}\alpha$  target at a scanning rate of  $4^\circ/\text{min}$ . Feature sizes of the microcrystalline structure of the semi-coke are represented by  $d_{002}$ ,  $L_a$ , and  $L_c$  and were solved according to the Scherrer formula and Bragg equation [30]:

$$d_{002} = \frac{\lambda}{2 \sin \theta_{002}}, \quad (4)$$

$$L_c = \frac{0.89\lambda}{\beta_{002} \cos \theta_{002}}, \quad (5)$$

where  $d_{002}$  is the distance between the single aromatic layers of the sample,  $L_c$  is the microcrystal stack height perpendicular to the aromatic lamellas,  $\theta_{002}$  is the glancing angle,  $\beta_{002}$  is the full width at half maximum of the diffraction peak, and  $\lambda$  is the wavelength at  $0.15406 \text{ nm}$  of the incident X-ray.

Functional group of semi-coke was detected through Fourier-transform infrared spectrometer (FTIR) (German Bruker, Vector 22). Semi-coke samples were prepared using the KBr squashing technique, and test spectral range was  $400\text{--}4,000 \text{ cm}^{-1}$  with a resolution ratio of  $4 \text{ cm}^{-1}$ . The sample spectra were obtained through scanning after deducting the blank KBr background. Aromaticity was derived using the formulas by Brown and Ladller [31]:

$$f_a = 1 - C_{\text{al}}/C, \quad (6)$$

$$C_{\text{al}}/C = [(H_{\text{al}}/H) \cdot (H/C)] / (H_{\text{al}}/C_{\text{al}}), \quad (7)$$

where  $C_{\text{al}}/C$  is the content of aliphatic carbon,  $H/C$  is the ratio of hydrogen/carbon numbers, which can be solved through elemental analysis,  $H_{\text{al}}/H$  is the proportion occupied by aliphatic hydrogen in total hydrogen,  $H_{\text{al}}/C_{\text{al}}$  is the carbon/hydrogen ratio in lipid groups and is taken as 1.8 for coal [31], and  $H_{\text{al}}$  is the aliphatic hydrogen, which can be solved by dividing the integral area  $A_{\text{al}}$  inside the wave band by the extinction coefficient  $a_{\text{al}}$  ( $a_{\text{al}}$  is taken as  $744 \text{ cm}^{-1}$  for semi-coke), as shown in Eq. 8:

$$H_{\text{al}} = \frac{A_{\text{al}}}{a_{\text{al}}}. \quad (8)$$

Physicochemical absorber (US Micromeritics, ASAP 2020M+C) and  $\text{N}_2$  adsorption method were used to test the specific surface area and micropore structure of semi-coke, with a degasification temperature during the test at  $200^\circ\text{C}$ .

### 3 Results and discussion

#### 3.1 Combustion/gasification reactivity

TG–DTG curves of combustion and gasification of semi-coke samples prepared under different pyrolytic

atmospheres are shown in Figure 2, and semi-coke combustion and gasification characteristic parameters are presented in Table 2.

As shown in Figure 2a, under air atmosphere, six semi-coke samples started losing weight under 368°C or higher, which indicated that volatiles in semi-coke have started to decompose. Subsequently, weight loss rate increased, which suggested that the fixed carbon experienced a rapid combustion reaction. Weight loss basically ended under 570°C or so, which indicated semi-coke after-combustion. In the initial phase of rapid combustion of six semi-coke samples, differences between TG and DTG curves were not evident. In the phase of maximum weight loss rate, the maximum combustion rates of different semi-coke were distinctive, with the reaction rate of char1 being the fastest, followed by char2; moreover, minor differences existed in the reaction rates of char3–char6. In the late combustion phase, DTG curves of semi-coke no. 2–6 slightly advanced. The range of ignition temperature of the six semi-coke samples was from 447°C to 455°C, which indicated that the differences in ignition temperature in the various semi-coke samples were poor. To compare the semi-coke combustion reactivity values, the six curves were analyzed through combustion reactivity indexes in Eq. 1. After calculation, semi-coke combustion reactivity indexes were sorted in descending order: char6 > char5 > char4 > char3 > char2 > char1, which indicated that compared with the pyrolysis atmosphere of N<sub>2</sub>, adding reducing gases CH<sub>4</sub> and H<sub>2</sub> in the pyrolysis process of raw coal will reduce the combustion reactivity and gasification reactivity of semi-coke.

Figure 2b indicates that under a CO<sub>2</sub> atmosphere, the six semi-coke samples experienced a volatile and slow gasification phase before 870°C or so, and a rapid gasification reaction happened under 870°C or so; moreover, the finishing temperature of gasification reaction was from 1,050°C to 1,100°C. The six semi-coke samples had noticeable differences in TG and DTG curves compared with char1 prepared under a nitrogen atmosphere;

furthermore, the TG and DTG curves of char2–char6 prepared after adding reducing gases experienced retrogression, and the maximum reaction rate and reaction finishing temperature escalated. The semi-coke gasification reactivity indexes were arranged in descending order: char6 > char5 > char4 > char3 > char2 > char1. The results indicated that the addition of reducing gases in the pyrolysis phase of raw coal resulted in a clear degradation of gasification reactivity and inhibition of composite gas of H<sub>2</sub>; in addition, CH<sub>4</sub> was the most recognizable, the influence of H<sub>2</sub> was stronger than that of CH<sub>4</sub>, and the increased concentration of reducing gases increased its inhibitory effect.

To compare the combustion and gasification reactivity of different semi-coke, time-dependent changes in carbon conversion rates of different semi-coke are illustrated in Figure 3. At the same combustion reaction time, the difference in combustion conversion rates of the different semi-coke was minimal. From Figure 3b, at the same gasification reaction time, different semi-coke had observable differences in gasification reactivity. The time required by char1 to complete combustion and gasification was 700 s or so, and that of char2–char6 continuously increased; thus, this phenomenon became increasingly apparent during gasification. This indicated that the pyrolytic atmosphere conditions influenced the gasification reactivity at a higher degree than that of combustion reactivity. The semi-coke has favorable combustion reactivity; therefore, the after-combustion temperature was lower than 600°C, and the chemical reaction itself could be the restrictive link of combustion. The semi-coke gasification reaction temperature was higher than that of the combustion reaction; moreover, the chemical reaction itself proceeded rapidly and the diffusion of reactants and products should be the restrictive link of this gasification process. Emphasis will be placed on the factors influencing semi-coke chemical reactions, such as carbon chemical structure, functional group distribution, and micropore structural characteristics that influence diffusion.

**Table 2:** Characteristic parameters of semi-coke during combustion and gasification processes

Samples	T <sub>max</sub> (°C)	V <sub>max</sub> (°C min <sup>-1</sup> )	T <sub>i</sub> (°C)	T <sub>f</sub> (°C)	R <sub>c</sub> (×10 <sup>3</sup> )	T <sub>0.5</sub> (°C)	R <sub>g</sub> (s <sup>-1</sup> [×10 <sup>4</sup> ])
char1	510	0.9915	447	574	2.21812	1,007	11.65501
char2	509	0.9396	454	567	2.0696	1,016	10.77586
char3	512	0.8657	447	559	1.93669	1,020	10.5042
char4	515	0.8468	448	572	1.89018	1,028	9.80392
char5	505	0.8106	450	579	1.80133	1,034	9.27644
char6	501	0.7875	455	570	1.73077	1,048	8.47458

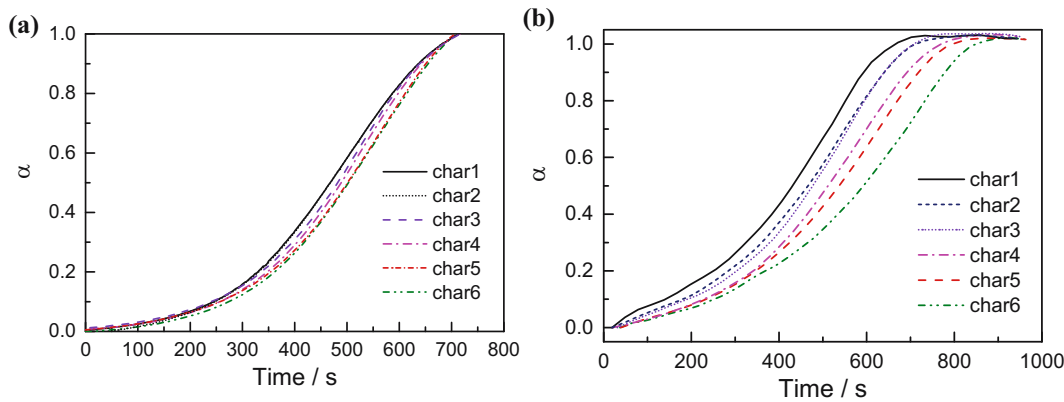


Figure 3: Time-dependent changes in carbon conversion rates of different semi-coke. (a) Air atmosphere; (b)  $\text{CO}_2$  atmosphere.

### 3.2 XRD analysis of chars

Figure 4 shows the XRD spectra of the six semi-coke samples. The  $\text{C}(002)$  peaks of samples char1-char6 sharpened, which indicated that the carbon microcrystalline structures of semi-coke prepared by adding reducing gases in the atmosphere were likely to be of the graphite state. X'Pert highscore analysis software, together with Eq. 4 and 5, was used to obtain the position of  $\text{C}(002)$  peak, lamellar spacing  $d_{002}$ , and aromatic lamella stack thickness  $L_c$ , and the results are listed in Table 3.

In Table 3, the differences in  $2\theta$  angle and  $d_{002}$  corresponding to the  $\text{C}(002)$  peaks of different semi-coke are unsatisfactory. However, the  $L_c$  values of char1-char6 gradually increased, thereby indicating that the aromatic lamella stack thickness of the semi-coke gradually expanded. The number of carbon stack lamellas increased, which indicated the enhancement of the pseudo-crystalline phase degree of semi-coke samples and further indicated the enhancement of the carbon ordering degree in the semi-coke. Adding the reducing gases in semi-coke pyrolysis

probably promoted the enhancement of the semi-coke graphitization degree because the hydrogen-free radicals generated by  $\text{H}_2$  and  $\text{CH}_4$  could permeate the semi-coke surface and would enhance the condensation of aromatic rings, thereby decreasing the number of available active sites [20–22].

Figure 5 shows the relationships of semi-coke  $L_c$  with the combustion and gasification reactivity indexes. As shown in Figure 5, semi-coke carbon microcrystalline structure has identical influence rules on combustion reactivity and gasification reactivity, namely, with the enhanced ordering degree of carbon microcrystalline structure, decreased semi-coke reactivity indexes, and the certain linear relation of the two. In a study on the influence of heat treatment temperature and heating rate on coke reactivity, Lu et al. found [24] that from amorphous carbon, the carbon structure described by the aromaticity and crystallite size became highly systematized with the rise in heat treatment temperature and decline in heating rate, thus, semi-coke reactivity was degraded. With the increased proportion of reducing gases in the nitrogen atmosphere, the semi-coke carbon structure became highly ordered, which degraded semi-coke reactivity because when the size of the aromatic lamella

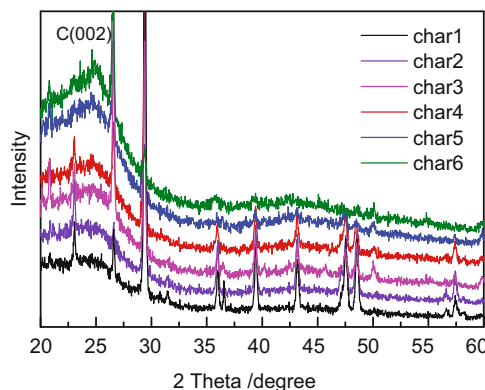


Figure 4: XRD spectra of different semi-cokes.

Table 3: Characteristic parameters of microcrystalline structure of semi-coke

Samples	$\text{C}(002)$ ( $^\circ$ )	$d_{002}$ ( $10^{-10} \text{ m}$ )	$L_c$ ( $10^{-10} \text{ m}$ )	$L_c (d_{002})$
char1	24.83	3.58	12.09	2.26
char2	24.91	3.57	12.21	2.20
char3	25.01	3.56	12.26	2.32
char4	25.02	3.56	12.39	2.36
char5	25.03	3.56	12.50	2.39
char6	25.04	3.56	12.93	2.51

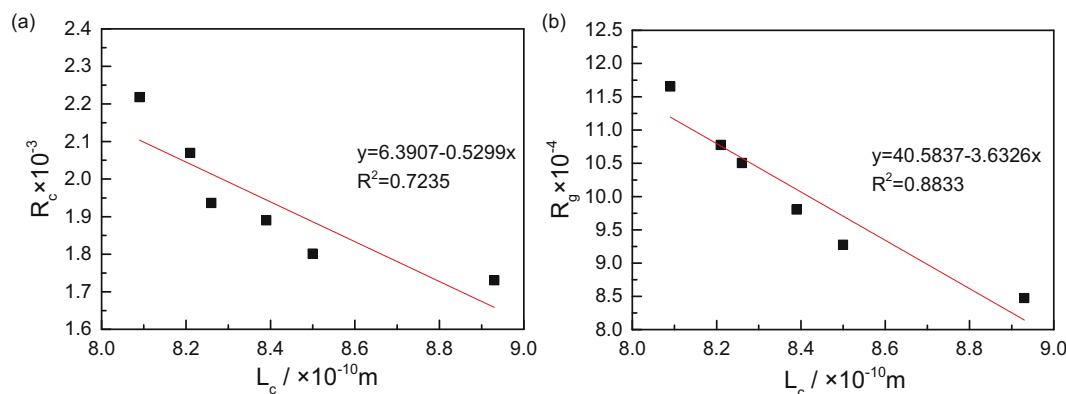


Figure 5: Relationships of semi-coke  $L_c$  with combustion and gasification reactivity indexes. (a)  $L_c$  vs  $R_c$ ; (b)  $L_c$  vs  $R_g$ .

increased, the ratio of the active marginal carbon atoms to the non-active carbon atoms in the cardinal plane will be reduced [32]. Moreover, when the arrangement of the aromatic lamellas became organized, the active carbon atoms bonded with the defects and the hetero atoms were reduced [21]. Both could degrade semi-coke combustion and gasification reactivity.

### 3.3 FTIR analysis of chars

Figure 6 shows the FTIR spectra of different semi-coke. To carry out specific analysis on the wave number region of semi-coke 4,000–400  $\text{cm}^{-1}$ , the entire infrared spectrum is divided into four parts [31] as follows: hydroxyl absorption peak (3,600–3,000  $\text{cm}^{-1}$ ), aliphatic hydrocarbon absorption peak (3,000–2,700  $\text{cm}^{-1}$ ), oxygen-containing functional group absorption peak (1,800–1,000  $\text{cm}^{-1}$ ), and aromatic hydrocarbon absorption peak (900–700  $\text{cm}^{-1}$ ). It can be seen from Figure 6 that the distribution of functional groups in different semi-coke samples is different. Compared with other semi-coke samples, there is an obvious hydroxyl absorption peak between char1 and char2, but char2 is mainly composed of free hydroxyl groups, char1 is mainly composed of phenol, alcohol, carboxylic acid, and hydroxyl in water, and there are obvious antisymmetric stretching vibrations of  $\text{CH}_3$  and  $\text{CH}_2$  in naphthalenes or aliphatic groups. All the semi-coke samples had stretching vibration of S–H bond near 2,510  $\text{cm}^{-1}$ , but the vibration peak shape of char1 was not obvious.  $\text{CH}_3$  vibration peak exists in all samples near 1,440  $\text{cm}^{-1}$ , but obvious vibration peak exists in char1 and char2 near 1,590  $\text{cm}^{-1}$ . This is the vibration peak of aromatic C=C, and it is the skeleton vibration of benzene ring. char1–char6 have obvious characteristic peaks near 880 and 710  $\text{cm}^{-1}$ , but the peak intensity of

char1 is significantly lower than that of other semi-focal points. char1 has obvious vibration peaks at 1,058 and 1,183  $\text{cm}^{-1}$ , which are stretching vibration peaks of Si–O–Si, Si=O, or Si–O–C. Oxygen-containing functional groups are obvious in char1. When the pyrolytic atmosphere contains  $\text{H}_2$  or  $\text{CH}_4$ , removal of hydroxyls and oxygen-containing functional groups reduced content of

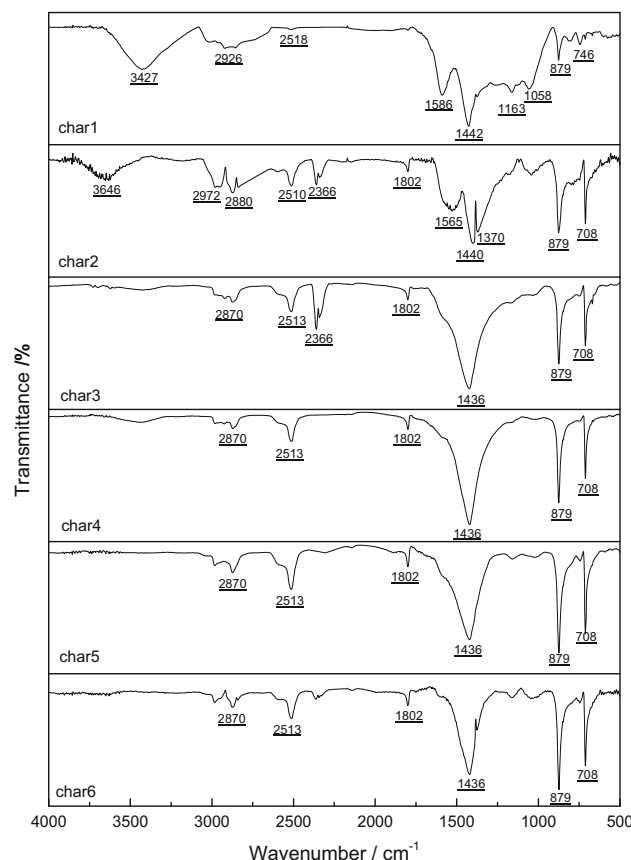


Figure 6: Semi-coke FTIR spectra.

**Table 4:** Structure parameters deduced from FTIR for chars

Samples	$H_{al}$ (%)	$H_{al}/H$	$C_{al}/C$	$f_a$
char1	0.789	0.326	0.05261	0.94739
char2	0.559	0.277	0.04344	0.95656
char3	0.497	0.266	0.04051	0.95949
char4	0.412	0.184	0.04869	0.95131
char5	0.37	0.184	0.04336	0.95664
char6	0.359	0.184	0.04228	0.95772

unsaturated side chains, and elevated condensation degree of macromolecular network will be facilitated.

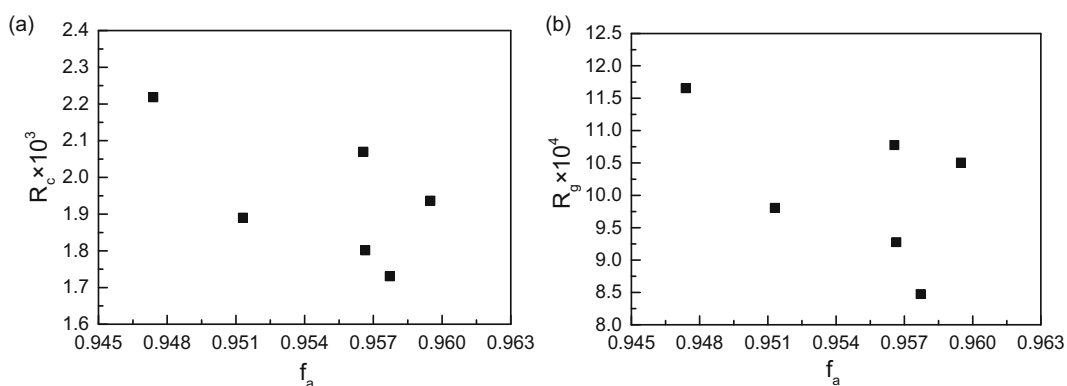
To further describe the differences in various semi-coke samples in the macromolecular structure, Eq. 6–8 were used to calculate and compare the aromaticity of semi-coke. Table 4 presents the obtained IR structural parameters. It can be seen from the table that when  $\text{CH}_4$  or  $\text{H}_2$  is added in the pyrolysis atmosphere, aliphatic hydrocarbons and carbon groups in the raw coal are more easily decomposed and precipitated, which is specifically reflected in the significant decrease in the contents of  $H_{al}$  and  $H_{ar}$  and the significant increase in  $f_a$  of the samples. However, the influence of  $\text{CH}_4$  atmosphere and  $\text{H}_2$  atmosphere is different. Compared with  $\text{H}_2$  atmosphere,  $\text{CH}_4$  atmosphere has a more obvious effect on  $f_a$  promotion.

Relationships of semi-coke aromaticity with combustion and gasification reactions are shown in Figure 7. There is no obvious relationship between the aromaticity and combustion and gasification reaction index, but char1 gasification reactivity and combustion reactivity are best, its corresponding  $f_a$  also minimum, shows that  $\text{N}_2$  pyrolysis atmosphere compared to add  $\text{CH}_4$  and  $\text{H}_2$ , can maintain the sample in a certain amount of reactive strong aliphatic group, inhibit samples influence the reactivity of the increase of aromatic carbon.

In summary, when  $\text{CH}_4$  or  $\text{H}_2$  is added in the pyrolysis atmosphere, aliphatic hydrocarbons and carbon groups in raw coal are more easily decomposed and precipitated, so as to improve the  $f_a$  of semi-coke and reduce the reactivity of semi-coke. The influence of its functional groups is manifested in the fact that hydroxyl group,  $\text{C}=\text{C}$ , and oxygen-containing functional groups have a promoting effect on the improvement of reactivity, whereas the increase in S–H and aromatic hydrocarbon contributes to the improvement of aromaticity, thus reducing the reactivity of semi-coke.

### 3.4 Effects of pore structure of chars on reactivity

Figure 8 shows the pore structural distribution of the six semi-coke samples. Figure 8a shows that micropores below 2 nm and mesopores at 2–50 nm contributes to the main specific surface area. Independent addition of  $\text{H}_2$  or  $\text{CH}_4$  to the pyrolytic atmosphere increased the specific surface area of semi-coke micropores, and the micro-pore-specific surface areas of char2 and char3 added with  $\text{CH}_4$  gas were significantly enlarged. Differences in specific surface area between semi-coke mesopores were visible, and the independent addition of  $\text{H}_2$  or  $\text{CH}_4$  in pyrolytic atmosphere reduced the specific surface area of the semi-coke mesopores. Mesopore-specific surface areas of char3 and char4 added with  $\text{H}_2$  gas decreased more evidently than those of char2 and char3 added with  $\text{CH}_4$  gas, and the specific surface areas of mesopores added with both  $\text{H}_2$  and  $\text{CH}_4$  were mostly reduced. Mesopores contributed to the main pore volume and the order of pore volumes of the different semi-coke was consistent with rule of specific surface area. The difference between

**Figure 7:** Relationships of semi-coke  $f_a$  with combustion and gasification reactivity indexes. (a)  $f_a$  vs  $R_c$ ; (b)  $f_a$  vs  $R_g$ .

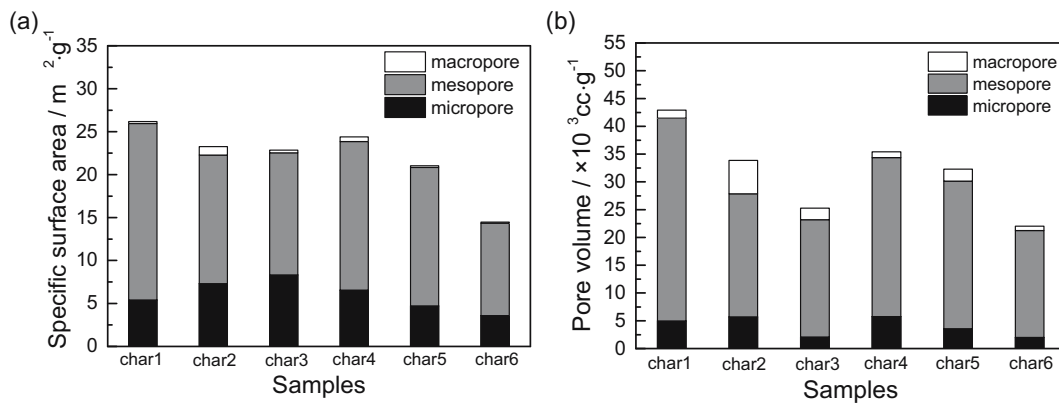


Figure 8: Specific surface area and pore volume of semi-coke.

micropores in terms of pore volume was not obvious, and pore volumes 50 nm above pores were small. The above results showed that the main pore structural types of semi-coke were micropores and mesopores; moreover, the influence of the regularity of the pyrolytic atmosphere on micropores was not strong, but the pyrolytic atmosphere could reduce the quantity of mesopores. This is because, with an elevated pyrolysis degree, the generation of micropores, which dominated the semi-coke-specific surface area, was reduced. Moreover, the  $\text{CH}_4$  and  $\text{H}_2$  in the pyrolytic atmosphere reacted with macromolecular side chains in the coal during pyrolysis to improve the yield and precipitation rate of pyrolytic gases [33], which then further boosted the development and growth of

micropores toward mesopores, as well as the cross-linking and combination of mesopores. As a result, the pore-specific surface area and pore volume were reduced.

Figures 9 and 10 show the relationships between semi-coke-specific surface area and combustion and gasification reactivity indexes. Combustion and gasification reactivity indexes presented weak linear correlations with micropore-specific surface area and pore volume. However, they have a favorable linear correlation with mesopore volume (i.e., as mesopore-specific surface area and pore volume increased, the combustion and gasification reactivity were improved) because compared with homogeneous reaction, as heterogeneous reaction processes, the semi-coke combustion and gasification

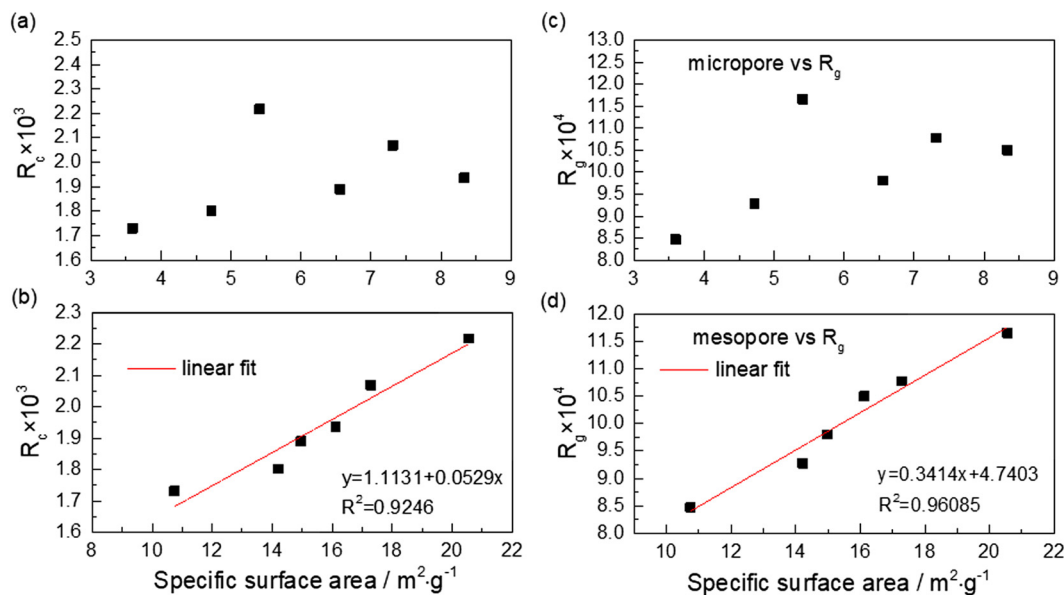
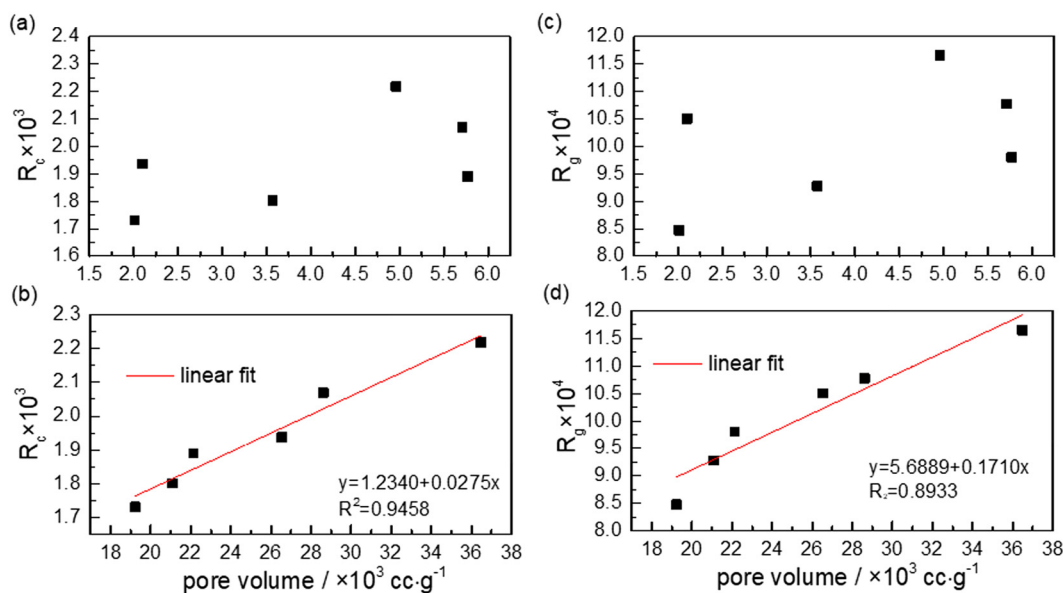


Figure 9: Relationships between semi-coke-specific surface area and reactivity indexes. (a) Micropore vs  $R_c$ ; (b) mesopore vs  $R_c$ ; (c) micropore vs  $R_g$ ; (d) mesopore vs  $R_g$ .



**Figure 10:** Relationships between semi-coke pore volume and reactivity indexes. (a) Micropore vs  $R_c$ ; (b) mesopore vs  $R_c$ ; (c) micropore vs  $R_g$ ; (d) mesopore vs  $R_g$ .

contained two important features, namely diffusion of reactant molecules and reaction interface conditions. Semi-coke pore structure not only provided a diffusion channel for oxygen/carbon dioxide molecules that is required by combustion and gasification but also provided a large specific surface area for gas analysis and solid contact during gas–solid heterogeneous reaction [28]. Therefore, the developed pore structure of semi-coke improved their combustion and gasification reactivity.

Semi-coke combustion and gasification reactivity were closely related to the ordering degree of carbon chemical structure and micropore structure; moreover, they had a certain relationship with the distribution of functional groups. For the convenience of semi-coke application in iron-making, the pyrolysis temperature, holding time, heating rate, and other conditional parameters during pyrolysis should be reasonably regulated to counterbalance the adverse effects of reducing gases in the pyrolytic atmosphere on the semi-coke reactivity, so that they meet blast furnace PCI requirements.

## 4 Conclusions

In this research, the combustion and gasification characteristics of semi-coke prepared under pyrolytic atmospheres rich in  $\text{CH}_4$  and  $\text{H}_2$  at different proportions were investigated, and the effect of carbon chemical structure, functional groups, and micropore structure of char on

reactivity was also analyzed. The results showed that  $\text{CH}_4$  and  $\text{H}_2$  exhibited inhibiting effect on semi-coke reactivity. This inhibiting effect on gasification reactivity was stronger than that of combustion reactivity, and the influence of  $\text{H}_2$  was stronger than that of  $\text{CH}_4$ . The reducing gases in the atmosphere enhanced the disordering degree of the carbon crystalline structure, boosted removal of hydroxyl and oxygen-containing functional groups, reduced content of unsaturated side chains, and elevated the condensation degree of the macromolecular network. The main semi-coke pore structural types were micropores and mesopores. Influence on the regularity of the pyrolytic atmosphere on micropores was not strong, but the pyrolytic atmosphere could inhibit mesopore development. Aromatic lamella stack height of the semi-coke, specific surface area of mesopore, and pore volume had favorable linear correlations with semi-coke reactivity indexes.

**Research funding:** The authors are grateful for the support of the National Natural Science Foundation of China (No. 51904223), the Natural Science Foundation Research Project of Shaanxi, China (No. 2020JQ-674), and the Science and Technology Plan of Yulin (No. Z20200396 and Z20200397).

**Author contributions:** Yuan She: writing – original draft, review and editing, methodology, formal analysis; Chong Zou: writing – review and editing, methodology; Shiwei Liu: formal analysis; Keng Wu: methodology, project

administration; Hao Wu: visualization, formal analysis; Hongzhou Ma: project administration; Ruimeng Shi: resources.

**Conflict of interest:** The authors state no conflict of interest.

**Data availability statement:** All data generated or analyzed during this study are included in this published article.

## References

- [1] Blesa MJ, Miranda JL, Moliner R, Lzquierdo MT, Palacios JM. Low-temperature co-pyrolysis of a low-rank coal and biomass to prepare smokeless fuel briquettes. *J Anal Appl Pyrolysis*. 2003;70(2):665–77. doi: 10.1016/S0165-2370(03)00047-0.
- [2] Wan X, Xing G, Wang Y. Development analysis of low-temperature pyrolysis technology for low rank coal. *Dry Technol Equip*. 2015;13(2):1–6. doi: 10.16575/j.cnki.issn1727-3080.2015.02.004.
- [3] Gupta S, Sahajwalla V, Al-Omari Y, French D. Influence of carbon structure and mineral association of coals on their combustion characteristics for pulverized coal injection (PCI) application. *Metall Mater Trans B*. 2006;37(3):457–73. doi: 10.1007/s11663-006-0030-y.
- [4] Osório E, Gomes MLI, Vilela ACF, Kalkreuth W, Almeida MA, Borrego AG, et al. Evaluation of petrology and reactivity of coal blends for use in pulverized coal injection (PCI). *Int J Coal Geol*. 2006;68(1–2):14–29. doi: 10.1016/j.coal.2005.11.007.
- [5] Wijayanta AT, Alam MS, Nakaso K, Fukai J, Kunitomo K, Shimizu M. Combustibility of biochar injected into the raceway of a blast furnace. *Fuel Process Technol*. 2014;117:53–9. doi: 10.1016/j.fuproc.2013.01.012.
- [6] Gupta S, Sahajwalla V, Wood J. Simultaneous combustion of waste plastics with coal for pulverized coal injection application. *Energy Fuels*. 2006;20(6):2557–63. doi: 10.1021/ef060271g.
- [7] Zhang LG, Ren W, Liu DJ, Zhang W, Wang ZY, Deng W. Study on semi-coke used as pulverized coal for injection into blast furnace. *Angang Technol*. 2015;1:13–17.
- [8] Yang SP, Cai WM, Zheng HA, Liang JQ, Zhang SJ, Xue QC. Performance analysis of semi-coke for blast furnace injection. *Chin J Process Eng*. 2014;14(5):896–900.
- [9] Xu CY, Dong J, Li XT, Tang AJ. Experimental research on semi-coke used for blast furnace injection and metallurgical performance. *J Iron Steel Res*. 2016;44(4):17–9.
- [10] Yang SP, Guo SQ, Zhang PH, Zhou JF, Wang M. Influence of semi-coke on blending coal injection characteristics for blast furnace. *J Iron Steel Res*. 2017;29(3):201–7. doi: 10.13228/j.boyuan.issn1001-0963.20160146.
- [11] Li PC, Zhang JL, Xu RS, Song TF. Representation of characteristics for modified coal, semi-coke and coke used in blast furnace injection. *Energy Metall Ind*. 2015;34(3):41–5.
- [12] He XM, Fu PR, Wang CX, Lin HT, Wu S, Cao SX. Combustion behavior of low rank coal char application in blast furnace injection. *Iron Steel*. 2014;49(9):92–6. doi: 10.13228/j.boyuan.issn0449-749x.20140066.
- [13] Haykiri-Açma H, Ersoy-Meriçboyu A, Küçükbayrak S. Combustion reactivity of different rank coals. *Energ Convers Manag*. 2002;43(4):459–65. doi: 10.1016/S0196-8904(01)00035-8.
- [14] Chen CH, Du SW, Yang TH. Volatile release and particle formation characteristics of injected pulverized coal in blast furnaces. *Energ Convers Manag*. 2007;48(7):2025–33. doi: 10.1016/j.enconman.2007.01.001.
- [15] Yu JL, Lucas JA, Wall TF. Formation of the structure of chars during devolatilization of pulverized coal and its thermoproperties: a review. *Prog Energy Combust Sci*. 2007;33(2):135–70. doi: 10.1016/j.pecs.2006.07.003.
- [16] Zou C, Wen LY, Zhang SF, Bai CG, Yin GL. Evaluation of catalytic combustion of pulverized coal for use in pulverized coal injection (PCI) and its influence on properties of unburnt chars. *Fuel Process Technol*. 2014;119:136–45. doi: 10.1016/j.fuproc.2013.10.022.
- [17] Cai HY, Guell AJ, Chatzakis IN, Lim JY, Dugwell DR, Kandiyoti R. Combustion reactivity and morphological change in coal chars: Effect of pyrolysis temperature, heating rate and pressure. *Fuel*. 1996;75(1):15–24. doi: 10.1016/0016-2361(94)00192-8.
- [18] Hu JH, Chen YQ, Qian KZ, Yang ZX, Yang HP, Li Y, et al. Evolution of char structure during mengdong coal pyrolysis: influence of temperature and  $K_2CO_3$ . *Fuel Process Technol*. 2017;159:178–86. doi: 10.1016/j.fuproc.2017.01.042.
- [19] Li Q, Wang ZH, He Y, Sun Q, Zhang YW, Kumar S, et al. Pyrolysis characteristic and evolution of char structure during pulverized coal pyrolysis in drop tube furnace: influence of temperature. *Energy Fuel*. 2017;31(5):4799–807. doi: 10.1021/acs.energyfuels.7b00002.
- [20] Colette BD, Cypres R, Fontana A, Hoegaerden M. Coal hydro-methanolysis with coke-oven gas: 2. Influence of the coke-oven gas components on pyrolysis yields. *Fuel*. 1995;74(1):17–9. doi: 10.1016/0016-2361(94)P4324-U.
- [21] Colette BD, Fontana A, Labani A, Laurent P. Coal hydro-methanolysis with coke-oven gas: 3. Influence of the coke-oven gas components on the char characteristics. *Fuel*. 1996;75(11):1274–8. doi: 10.1016/0016-2361(96)00108-1.
- [22] Liao HQ, Li BQ, Zhang BJ. Co-pyrolysis of coal with hydrogen-rich gases: 1. Coal pyrolysis under coke-oven gas and synthesis gas. *Fuel*. 1998;77(8):847–51. doi: 10.1016/S0016-2361(97)00257-3.
- [23] Zhong M, Ma F. Analysis of product distribution and quality for continuous pyrolysis of coal in different atmospheres. *J Fuel Chem Technol*. 2013;41(12):1427–36.
- [24] Lu LM, Sahajwalla V, Harris D. Coal char reactivity and structural evolution during combustion-factors influencing blast furnace pulverized coal injection operation. *Metall Mater Trans B*. 2001;32(5):811–20. doi: 10.1007/s11663-001-0068-9.
- [25] Dong XF, Pinson D, Zhang SJ, Yu AB, Zulli P. Gas-powder flow in blast furnace with different shapes of cohesive zone. *Appl Math Model*. 2006;30(11):1293–309. doi: 10.1016/j.apm.2006.03.004.

- [26] Suzuki T, Smoot LD, Fletcher TH, Smith PJ. Prediction of high-intensity pulverized coal combustion. *Combust Sci Technol.* 1986;45(3-4):167–83. doi: 10.1080/00102208608923848.
- [27] Gong XZ, Guo ZC, Wang Z. Reactivity of pulverized coals during combustion catalyzed by  $\text{CeO}_2$  and  $\text{Fe}_2\text{O}_3$ . *Combust Flame.* 2010;157(2):351–6. doi: 10.1016/j.combustflame.2009.06.025.
- [28] Liang P, Wang ZF, Bi JC. Process characteristics investigation of simulated circulating fluidized bed combustion combined with coal pyrolysis. *Fuel Process Technol.* 2007;88(1):23–8. doi: 10.1016/j.fuproc.2006.05.005.
- [29] Li XG, Ma BG, Xu L, Luo ZT, Wang K. Catalytic effect of metallic oxides on combustion behavior of high ash coal. *Energy Fuel.* 2007;21(5):2669–72. doi: 10.1021/ef070054v.
- [30] Kevin AD, Robert HH, Nancy YCY, Thomas H. Evolution of char chemistry, crystallinity, and ultrafine structure during pulverized-coal combustion. *Combust Flame.* 1995;100(1–2):31–40. doi: 10.1016/0010-2180(94)00062-W.
- [31] Li QZ, Lin BQ, Zhao CS, Wu WF. Chemical structure analysis of coal char surface based on Fourier-transform infrared spectrometer. *Proc CSEE.* 2011;31(32):46–52. doi: 10.1007/s12583-011-0163-z.
- [32] Lu LM, Kong CH, Sahajwalla V, Harris D. Char structural ordering during pyrolysis and combustion and its influence on char reactivity. *Fuel.* 2002;81(9):1215–25. doi: 10.1016/S0016-2361(02)00035-2.
- [33] Scaccia S, Calabò A, Mecozi R. Investigation of the evolved gases from Sulcis coal during pyrolysis under  $\text{N}_2$  and  $\text{H}_2$  atmospheres. *J Anal Appl Pyrolysis.* 2012;98(11):45–50. doi: 10.1016/j.jaap.2012.05.001.